

# Xyloketal derivative C53N protects against mild traumatic brain injury in mice

This article was published in the following Dove Medical Press journal:  
*Drug Design, Development and Therapy*

Fengyin Liang<sup>1</sup>  
Fengjuan Su<sup>1</sup>  
Xiaoxiao Wang<sup>2</sup>  
Simei Long<sup>1</sup>  
Yinglin Zheng<sup>3</sup>  
Xiaofei He<sup>1</sup>  
Jiyan Pang<sup>3</sup>  
Zhong Pei<sup>1</sup>

<sup>1</sup>Department of Neurology, Guangdong Provisional Key Laboratory for Diagnosis and Treatment of Major Neurological Diseases, The First Affiliated Hospital, Sun Yat-sen University, Guangzhou 510080, People's Republic of China; <sup>2</sup>Department of Medical Oncology, Sun Yat-sen University Cancer Center, Guangzhou 510060, People's Republic of China; <sup>3</sup>School of Chemistry, Sun Yat-sen University, Guangzhou 510275, People's Republic of China

**Purpose:** Mild traumatic brain injury (mTBI), the most common type of TBI, can result in prolonged cognitive impairment, mood disorders, and behavioral problems. Reducing oxidative stress and inflammation can rescue the neurons from mTBI-induced cell death. Xyloketal B, a natural product from mangrove fungus, has shown good antioxidative and neuroprotective effects in several disease models. Here, we investigated the potential protection afforded by a xyloketal derivative, C53N, in a closed-skull mTBI model.

**Materials and methods:** Skulls of mice were thinned to 20–30  $\mu\text{m}$  thickness, following which they were subjected to a slight compression injury to induce mTBI. One hour after TBI, mice were intraperitoneally injected with C53N, which was solubilized in 0.5% dimethyl sulfoxide in saline. In vivo two-photon laser scanning microscopy was used to image cell death in injured parenchyma in each mouse over a 12-hour period (at 1, 3, 6, and 12 hours). Water content and oxidation index, together with pathological analysis of glial reactivity, were assessed at 24 hours to determine the effect of C53N on mTBI.

**Results:** Cell death, oxidative stress, and glial reactivity increased in mTBI mice compared with sham-injured mice. Treatment with 40 or 100 mg/kg C53N 1 hour after mTBI significantly attenuated oxidative stress and glial reactivity and reduced parenchymal cell death at the acute phase after mTBI.

**Conclusion:** The present study highlights the therapeutic potential of the xyloketal derivative C53N for pharmacological intervention in mTBI.

**Keywords:** xyloketal derivative, mTBI, in vivo imaging, antioxidant activity, neuroprotective activity

## Introduction

Traumatic brain injury (TBI) is the leading cause of death and disability in young adults.<sup>1,2</sup> The mild form of TBI (mTBI) is the major type and constitutes around 80% of all TBIs.<sup>3</sup> Unlike moderate to severe forms of TBI, mTBI does not cause immediate severe symptoms. However, mTBI can result in prolonged cognitive impairment, mood disorders, and behavioral problems.<sup>4,5</sup> Currently, there is no effective treatment for patients with mTBI. Thus, there is an urgent need for development of effective treatments. Unfortunately, the underlying molecular and biochemical mechanisms of mTBI still remain elusive. Recently, clinical and experimental studies have revealed a critical role of oxidative stress and inflammation in the pathophysiology of mTBI.<sup>6,7</sup> mTBI induces excessive ROS and inflammation, which in turn disrupts the blood–brain barrier, causes neuronal cell death, and eventually leads to neurological dysfunction.<sup>8,9</sup> By contrast, reducing oxidative stress and inflammation can rescue the neurons from mTBI-induced cell death.<sup>10</sup>

Marine organisms are currently receiving much attention for drug development due to their tremendous biodiversity. Xyloketal B is one of a series of novel ketal

Correspondence: Zhong Pei  
Department of Neurology, Guangdong Provisional Key Laboratory for Diagnosis and Treatment of Major Neurological Diseases, The First Affiliated Hospital, Sun Yat-sen University, No 58 Zhongshan Road II, Guangzhou 510080, People's Republic of China  
Tel +86 20 8775 5766 ext 8282  
Fax +86 20 8733 5935  
Email peizhong@mail.sysu.edu.cn

Jiyan Pang  
School of Chemistry, Sun Yat-sen University, No 135, Xingang Xi Road, Guangzhou 510275, People's Republic of China  
Tel/fax +86 20 8403 6554  
Email cespjy@mail.sysu.edu.cn

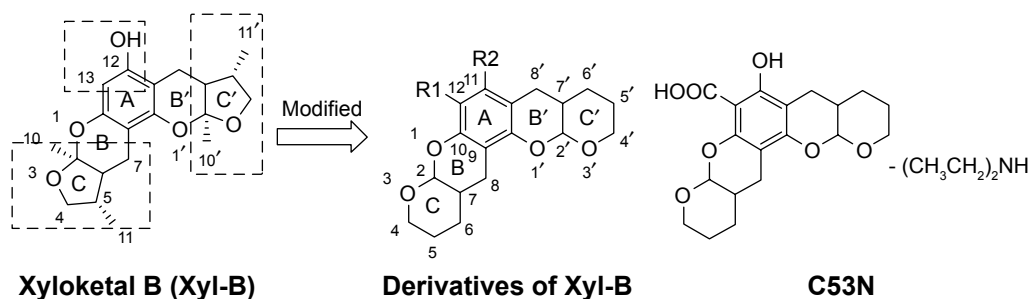


**Figure 1** Structures of xyloketal B and its derivatives (C53N).

compounds isolated from the mangrove fungus *Xylaria* sp. from the South China Sea.<sup>11,12</sup> Our previous studies have demonstrated that xyloketal B is a new antioxidant that has cardioprotective and neuroprotective actions.<sup>13–16</sup> However, several weaknesses of xyloketal B limit its application. First, protection against neural cell injury was moderate despite its good in vitro antioxidative activity. Moreover, asymmetric synthesis and modification of xyloketal B are difficult because of six asymmetric carbons at the 2, 2', 5, 5', 6, and 6' positions in its structure. In recent years, we have developed a series of analogs to improve xyloketal B. C53N, a derivative of xyloketal B, has demonstrated excellent antioxidative and neuroprotective effects in different disease models.<sup>14,17</sup> In addition, C53N can be easily synthesized with excellent yield. Structures of xyloketal B and its derivatives are shown in Figure 1.

In the present study, we examined the effects of the xyloketal derivative, C53N, in a closed-skull mTBI model. Using two-photon laser scanning microscopy, we assessed parenchymal cell death over 12 hours in live animals with mTBI.<sup>8,18</sup> Xyloketal derivative C53N was administered 1 hour after mTBI at 40 or 100 mg/kg. We examined cell death at 3-hour intervals within the initial 12 hours and evaluated oxidative stress and glial reactivity 24 hours after TBI. We found that C53N significantly attenuated oxidative stress and reduced parenchymal cell death in mice with mTBI. Thus, our data suggest that C53N has great potential to be developed as an effective neuroprotectant for mTBI.

## Materials and methods

### Chemicals and reagents

We synthesized and purified xyloketal derivative C53N in the School of Chemistry at Sun Yat-sen University, People's Republic of China, according to a previously reported method.<sup>14</sup>

Reduction of 3,4-dihydro-2*H*-pyran-5-carboxylate followed by electrophilic aromatic substitution with phloroglucinol carboxylic acid gave C53. C53 was purified by

flash chromatography (Pet:EtOAc=50:1–30:1), followed by crystallization to obtain the pure compound. A solution of C53 (0.2 g, 0.6 mmol) and diethylamine (0.2 g, 6 mmol) in acetone (20 mL) was stirred at room temperature for 30 minutes. Acetone and excess diethylamine were removed under reduced pressure with a rotary evaporator, leaving the C53N compound as a white foam, with a total yield of 58%. <sup>1</sup>H nuclear magnetic resonance (NMR) data were recorded on a 400 MB NMR spectrometer operating at 400 MHz for <sup>1</sup>H. HPLC and NMR spectroscopy showed that the purity of C53N was >95%; <sup>1</sup>H NMR (400 MHz, CDCl<sub>3</sub>) δ 5.31 (d, J=2.5 Hz, 1H), 5.25 (t, J=2.8 Hz, 1H), 4.13–3.90 (m, 2H), 3.76–3.54 (m, 2H), 3.00 (q, J=7.3 Hz, 4H), 2.74–2.54 (m, 4H), 2.16 (s, 1H), 2.15–2.08 (m, 2H), 1.79–1.54 (m, 8H), 1.29 (t, J=7.3 Hz, 6H).

We dissolved the compound in dimethyl sulfoxide (DMSO) and stored it at 4°C until use. We purchased all other reagents from Sigma-Aldrich (St Louis, MO, USA), unless otherwise specified.

### Mice and drug administration

Male C57BL/6 mice (3 months old, weighing 20–25 g) were purchased from Guangdong Medical Laboratory Animal Center, People's Republic of China. Animal care and experimental procedures were performed in strict accordance with the National Institutes of Health Guide for the Care and Use of Laboratory Animals. Animal experiments were approved by the Ethical Committee on Animal Experimentation of The First Affiliated Hospital, Sun Yat-sen University, People's Republic of China. The animal ethics number was [2017] 060.

Animals were randomly divided into four groups (n=5–7 per group) as follows:

- Group 1: sham mice with a thinned skull, but without compression TBI that received vehicle only (0.5% DMSO in saline) by intraperitoneal injection
- Group 2: mTBI mice that received vehicle only (0.5% DMSO in saline) by intraperitoneal injection 1 hour after compression injury

- Group 3: mTBI mice that received 40 mg/kg C53N in 0.5% DMSO by intraperitoneal injection 1 hour after compression injury
- Group 4: mTBI mice that received 100 mg/kg C53N in 0.5% DMSO by intraperitoneal injection 1 hour after compression injury.

## mTBI preparation

Animals were deeply anesthetized with 5% isoflurane, and anesthetization was maintained with 2% isoflurane in a mixture of 20% oxygen and 80% air. We used a regulated heating pad (Reward, Shenzhen, People's Republic of China) to maintain the rectal temperature of the animals at  $37^{\circ}\text{C}\pm 0.5^{\circ}\text{C}$ .

We placed the animals in a stereotaxic apparatus and used a sterile scalpel to cut an incision through the midline skin of the skull to expose the bone. We used a microdrill to create a 2.0×2.0 mm thinned cranial window over the left somatosensory cortex. The cranial window was located between bregma and lambda sutures. We induced compression injury according to a previous report,<sup>18</sup> with some modifications. Briefly, we thinned the skull for 1–2 minutes to a thickness of 20–30  $\mu\text{m}$ . Under stereotactic guidance, we then gently pressed the pliable skull bone downward 0.5 mm to create a constant concavity in the bone using the blunt end (~1.0 mm width) of a surgical instrument, such that the pliable skull bone compressed the surface of the brain.

## Transcranial propidium iodide staining

Transcranial application of propidium iodide (PI; Sigma-Aldrich) has been used to reliably label dead cells in the meninges and parenchyma through the intact, thinned skull.<sup>8</sup> Therefore, we used PI to assess cell death at the compression site at 1, 3, 6, and 12 hours after injury in each mouse. Briefly, PI (1.5 mM) in artificial cerebrospinal fluid was placed on the thinned skull for 30 minutes at each time point. After a single wash with artificial cerebrospinal fluid, brain cortex was imaged by two-photon microscopy.

For lesion volume detection, PI was administered by transcranial application over the compression site for 30 minutes before fixation at 24 hours. The total number of PI-positive cells in the focal lesion was calculated using the ImageJ software (NIH, Bethesda, MD, USA) “analyze particles” tool.

## Labeling of blood vessels

At the same time points as the PI staining mentioned above, 0.2 mL of 2% (wt/vol) solution of 2 MDa fluorescein-dextran (FD2000S; Sigma-Aldrich) in saline was administered intravenously to each mouse to label the blood vessels fluorescent green.

## In vivo two-photon imaging

To conduct in vivo two-photon imaging, we fixed the mouse in a custom-fabricated metal frame that held its head with cyanoacrylate and dental cement. The animal was then placed on the stage of a Leica DM6000 CFS (Leica Microsystems, Wetzlar, Germany). Leica LAS AF 2.5 software was used for laser scanning and data acquisition. All images were acquired using two-channel non-descanned detector detection, with emission filters of 525/50 and 585/50 nm, on a TCS SP5 MP System (Leica Microsystems). A Leica NA 0.95, 25× water immersion objective was used to visualize the vascular network and dead cells. Cells labeled by PI (exhibiting red fluorescence) were defined as dead cells and blood vessels were labeled green. Stacks of images were acquired using a step size of 2.0  $\mu\text{m}$  to a depth of 300  $\mu\text{m}$ .

## Lesion volume calculation

Lesion volumes were calculated by PI staining according to published literature.<sup>19</sup> Briefly, we sliced fixed brains into 50  $\mu\text{m}$  thick sections, captured images of the lesion site by confocal microscopy, and measured the lesion volume using ImageJ software. The total infarct volume was defined as the sum of the PI staining volumes.

## Brain edema measurement

The percentage brain water content was determined using the wet–dry method. The percentage water content (%  $\text{H}_2\text{O}$ ) was calculated for each hemisphere as follows: %  $\text{H}_2\text{O}$  = [(wet weight – dry weight)/wet weight] × 100%.

## ROS test and glutathione (GSH) measurement

We used commercial kits to assess ROS (Hydrogen Peroxide Assay Kit S0038; Beyotime) and GSH (Cellular Glutathione Peroxidase Assay Kit S0056; Beyotime) levels based on the protocols provided by the manufacturer. Briefly, we perfused the injured cortex with 0.9% saline (100  $\mu\text{L}$ /10 mg tissue) and extracted brain tissue in a tissue homogenizer instrument (SANYO, MSS.150-CX15) at 24 hours postinjury. We then mixed the tissue by vortexing, followed by centrifugation at 14,000 rpm for 5 minutes. We collected the supernatant and diluted with tissue lysates. The concentrations of ROS and GSH were evaluated by measurement of the absorbance at 560 nm for ROS and 420 nm for GSH.

## Histological analysis

The brain regions under the thinned skull window from each brain were dissected into 10  $\mu\text{m}$  thick serial coronal slices.

The following cell types were labeled: neurons (anti-NeuN; 1:400; EMD Millipore, Billerica, MA, USA), astrocytes (anti-GFAP; 1:400; Sigma-Aldrich), and microglia (anti-Iba1; 1:400; Wako, Osaka, Japan). Two-dimensional images were captured from the stained frozen sections using a Leica SP5 confocal microscope equipped with a 25× objective. Images were collected using sequential scanning with the 405, 488, and 561 nm lasers to produce combined overlays.

## Statistical analysis

SPSS version 22.0 (IBM Corporation, Armonk, NY, USA) was used for statistical analysis. Shapiro–Wilk test was used to check data distribution. Parametric tests (Student's *t*-test and ANOVA) were applied as data were found to be normally distributed. *P*-values below 0.05 were considered statistically significant.

## Results

### Synthesis of xyloketal derivative C53N

Xyloketal derivative C53N was synthesized according to a previously reported method.<sup>14</sup> Reduction of 3,4-dihydro-2*H*-pyran-5-carboxylate was followed by electrophilic aromatic substitution with phloroglucinol carboxylic acid to give C53. C53N is a diethylamine salt of C53, which has improved water solubility. The scheme for synthesis of C53N is shown in Figure 2.

C53 was purified by flash chromatography (Pet:EtOAc=50:1–30:1), followed by crystallization to obtain the pure compound. A solution of C53 (0.2 g, 0.6 mmol) and diethylamine (0.2 g, 6 mmol) in acetone (20 mL) was stirred at room temperature for 30 minutes. Acetone and excess diethylamine were removed under reduced pressure with a rotary evaporator to leave the C53N compound as a white foam, with a total yield of 58%.

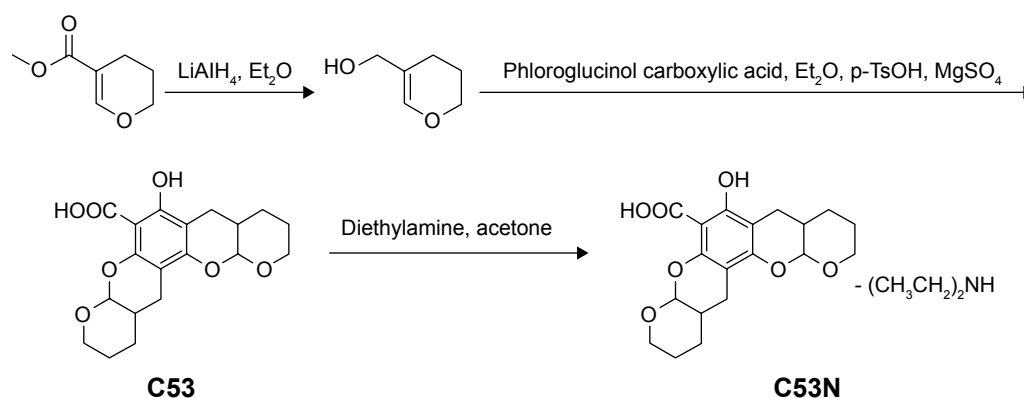


Figure 2 Scheme for synthesis of C53N.

### Xyloketal derivative C53N reduced cell death after mTBI

We evaluated the effects of C53N in a closed-skull mTBI model. PI was used to label dead cells at 1, 3, 6, and 12 hours after compression brain injury. Leica software (LAS AF Lite) was used to reconstruct stacks of images into three-dimensional vasculature images (Figure 3A). PI-positive dead cells were evident in the parenchyma in all the animals with compression injury, while there were no dead cells in the brain parenchyma of sham mice. Figure 3B shows images of the plane 100  $\mu\text{m}$  below the meninges at each time point, which correspond to the images in Figure 3A. Compared with vehicle-treated animals, the number of dead cells was significantly lower at 6 or 12 hours following mTBI in animals receiving 40 or 100 mg/kg xyloketal derivative C53N ( $P < 0.05$ ; Figure 3C). Our data suggest that C53N reduces brain cell death during acute brain injury.

### Xyloketal derivative C53N reduced lesion size post-mTBI

Lesion volume was evaluated according to cell death by PI staining 24 hours post-mTBI. As shown in Figure 4A, dead cells and neuronal loss were observed in the injury site in all TBI mice, while there were no PI-positive cells in sham mice. Mice treated with xyloketal derivative C53N showed significantly reduced cell death and neuronal loss in the cortex compared with vehicle-treated mice after mTBI (Figure 4B).

### Xyloketal derivative C53N decreases edema 24 hours post-mTBI

As shown in Figure 5, following mTBI, the brain injury site had a higher percentage of water content compared with sham mice. In mice treated with 40 mg/kg C53N, the water content was significantly lower than in mice treated with vehicle.



The water content was also significantly lower in mice treated with 100 mg/kg C53N compared with mice treated with vehicle. These data imply that the xyloketal derivative C53N decreases edema 24 hours post-mTBI.

### Xyloketal derivative C53N reduces ROS and increases GSH post-mTBI

We used commercial kits to measure the levels of  $H_2O_2$ , a potent ROS species, and GSH in injured cortex at 24 hours postinjury. We found that ROS, as evidenced by  $H_2O_2$ , was >2.5 times higher in mTBI mice than in sham

mice ( $P<0.01$ ), but animals that received different doses of xyloketal derivative C53N had decreased  $H_2O_2$  in the injury site compared with vehicle-treated mice (Figure 6A). In addition, as shown in Figure 6B, GSH in mTBI mice was 68.4% of that in sham mice. There was no difference in the concentration of GSH in mice treated with 40 mg/kg xyloketal derivative C53N, but mice that received 100 mg/kg xyloketal derivative C53N had an increased concentration of GSH compared with vehicle-treated mice ( $*P<0.01$ ). Thus, the present study indicates that xyloketal derivative C53N protects against mTBI at least partly through its antioxidant action.

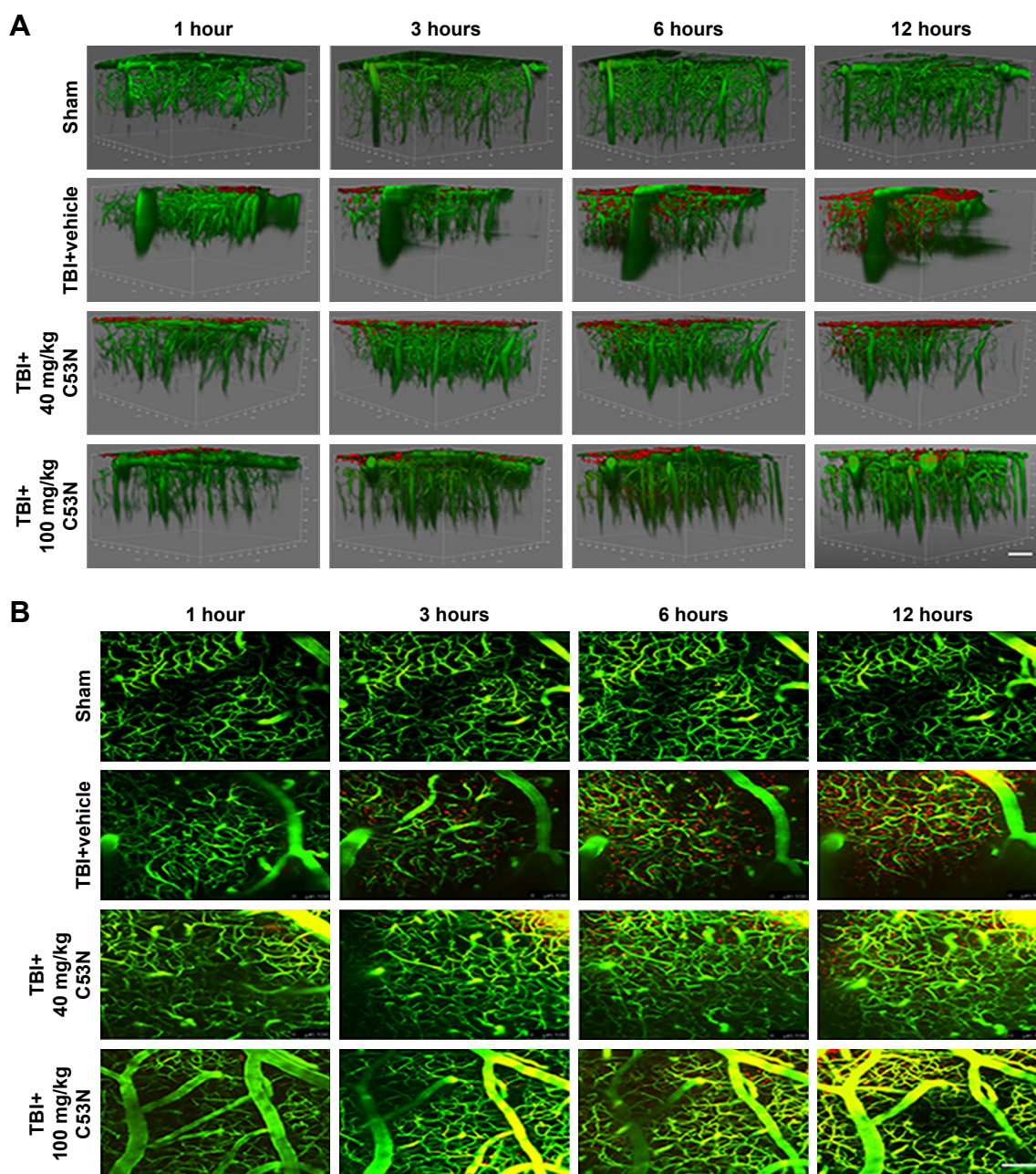
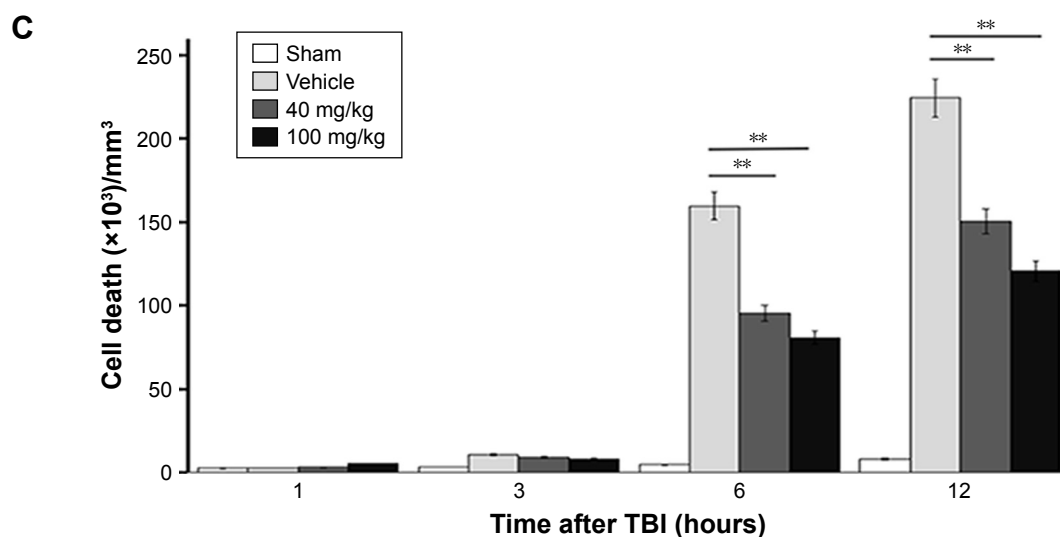


Figure 3 (Continued)



**Figure 3** PI labeling of cell death in live animals after mild compression injury.

**Notes:** (A) Cell death in the brain parenchyma after mild compression injury in representative reconstructed three-dimensional brain vascular images produced by two-photon laser microscopy. The vascular network was displayed using 200 kD FITC dextran (green fluorescence) and dead cells were labeled by transcranially applied PI (red fluorescence). (B) Images of the plane 100  $\mu$ m below the meninges at each time point, which correspond to the images in A. Scale bar: 100  $\mu$ m for A and 200  $\mu$ m for B. (C) Quantification of cell death in the parenchyma at 1, 3, 6, and 12 hours after mild compression injury (mean $\pm$ SEM). The number of PI<sup>+</sup> dead cells (per mm<sup>3</sup>) was significantly lower in animals with different doses of xyloketal derivative C53N compared with vehicle-treated animals at 6 and 12 hours (\*\* $P$ <0.01). All data are representative of  $n=6$  mice per group.

**Abbreviations:** FITC, fluorescein isothiocyanate; PI, propidium iodide; SEM, standard error of the mean; TBI, traumatic brain injury.

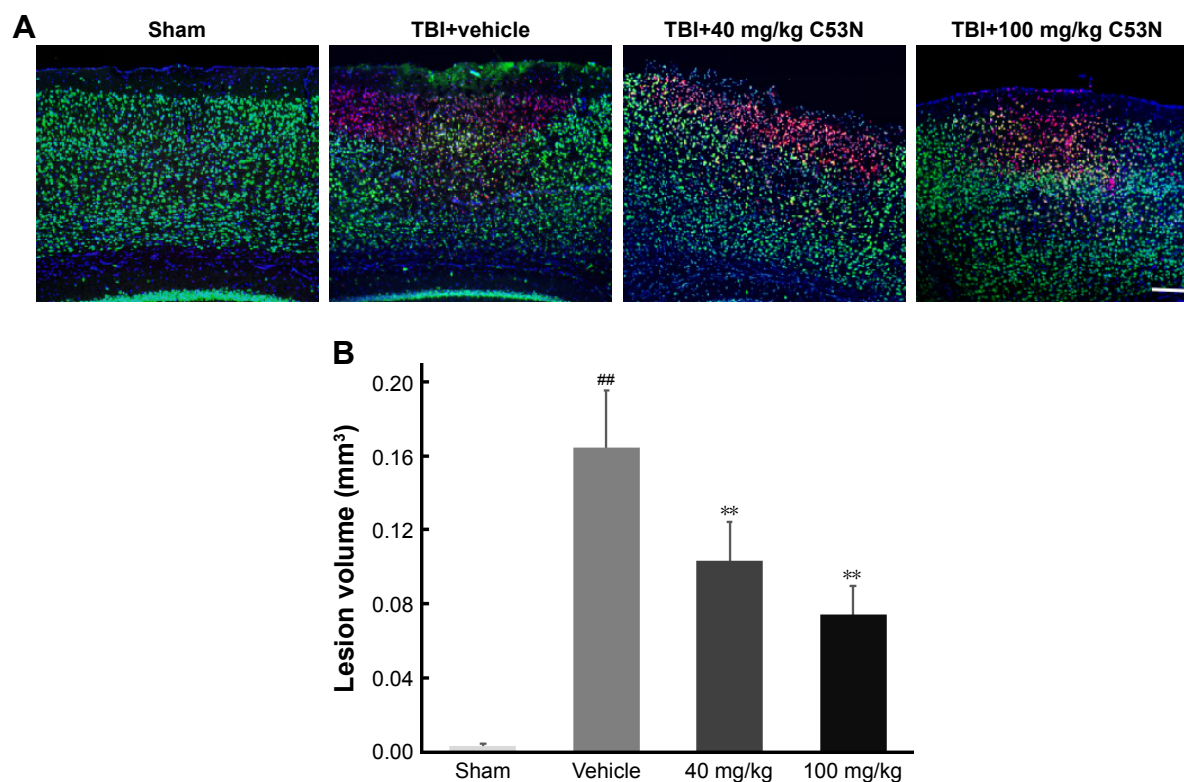


**Figure 4** Brain lesion volume evaluation 24 hours post-mTBI.

**Notes:** (A) Brain lesions in representative photographs of immunofluorescence staining. Dead cells were labeled by transcranially applying PI 30 minutes before fixation. Dead cells (labeled by PI), neurons (labeled by anti-NeuN antibody), and cell nuclei (labeled by DAPI) are shown in red, green, and blue, respectively. Scale bar: 100  $\mu$ m for A. (B) Post-traumatic lesion volume was quantified. Lesion volume was notable in vehicle-treated mice compared with sham mice 24 hours after TBI (## $P$ <0.01). However, the lesion volume was significantly lower in animals receiving xyloketal derivative C53N at 40 mg/kg (0.11 $\pm$ 0.02 mm<sup>3</sup>) or 100 mg/kg (0.07 $\pm$ 0.02 mm<sup>3</sup>) compared with vehicle-treated animals (0.14 $\pm$ 0.03 mm<sup>3</sup>); \*\* $P$ <0.01;  $n=6$  per group.

**Abbreviations:** mTBI, mild form of traumatic brain injury; PI, propidium iodide.

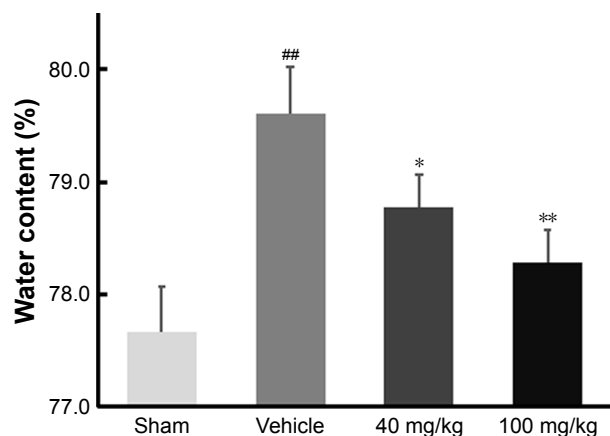


**Figure 5** Brain water content evaluation 24 hours post-TBI.

**Notes:** The water content in the cortex of sham mice was  $77.66\pm 0.41\%$ , while mTBI-induced water content ( $79.60\pm 0.42\%$ ) was significantly increased in the injury site compared with sham mice ( $^{###}P<0.01$ ). The water content of mice treated with 40 mg/kg C53N 1 hour after mTBI was  $78.78\pm 0.29\%$ , which was significantly lower than that of mice treated with vehicle ( $^{*}P<0.05$ ). The water content of mice treated with 100 mg/kg C53N 1 hour after mTBI was  $78.28\pm 0.29\%$ , which was also significantly lower than that of mice treated with vehicle ( $^{**}P<0.01$ );  $n=6$  per group. **Abbreviations:** mTBI, mild form of traumatic brain injury; PI, propidium iodide; TBI, traumatic brain injury.

## Xyloketal derivative C53N decreases glial activity post-mTBI

To investigate whether the xyloketal derivative C53N can act on neuroinflammation after TBI, we examined reactive astrocytes and microglia using anti-GFAP and anti-IBA1 antibodies, respectively. As shown in Figure 7A and B, few GFAP-positive astrocytes were detected in sham mice. However, GFAP-positive astrocytes were evident at 24 hours

post-trauma. By contrast, the xyloketal derivative C53N at 40 or 100 mg/kg significantly decreased the number of astrocytes at 24 hours compared with vehicle treatment ( $P<0.05$ ). As shown in Figure 7C and D, microglia were scattered in the cortex of sham mice. These microglia exhibited the features of quiescent microglia, including small cell bodies and fine, ramified processes (Figure 7E). However, Iba1-positive microglia were evident at 24 hours post-trauma. The morphology of microglia in the injured cortex resembled microglial reactive-like phenotypes, such as an amoeboid shape with large cell bodies and thickened, short processes (Figure 7E). Administration of xyloketal derivative C53N at 100 or 40 mg/kg significantly inhibited Iba1-positive microglia post-trauma ( $P<0.05$ ; Figure 7D) and attenuated the microglial reactive-like phenotype to a lesser degree. Thus, the present data suggest that the xyloketal derivative C53N significantly decreases glial activity post-mTBI.

## Discussion

The mTBI is frequently underestimated as the immediate physical symptoms decrease rapidly and conventional neuroimaging studies often do not show visible evidence of brain lesions. In the present study, we used a balance beam and Rotarod to test the functional outcome of mice at 24 hours after mTBI; however, there were no differences between mTBI and sham mice (data not shown). This is probably because it was such a small TBI that functional damage would not be evident within a short space of time. A more

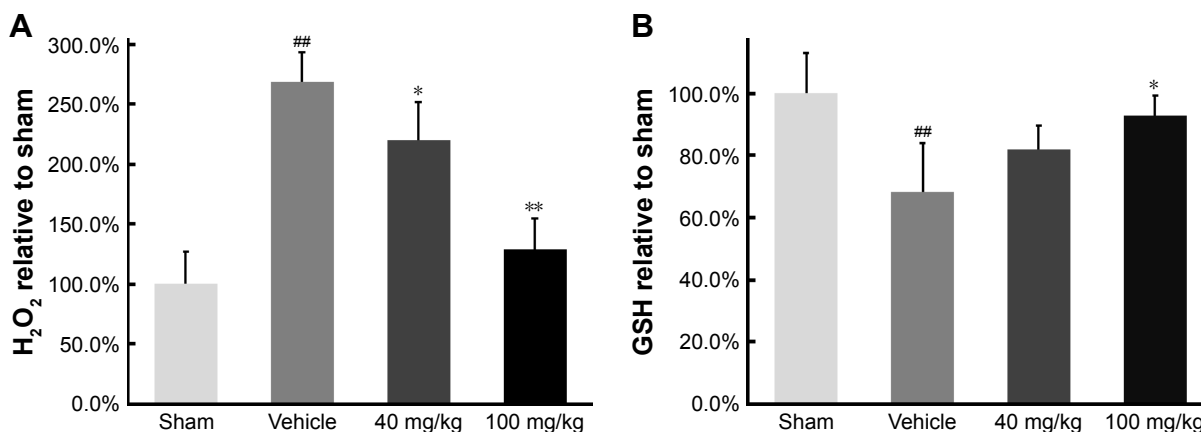


**Figure 6** Increased generation of H<sub>2</sub>O<sub>2</sub> and GSH in the mice.

**Notes:** (A) A hydrogen peroxide assay kit was used to quantify H<sub>2</sub>O<sub>2</sub> concentration. The concentration of H<sub>2</sub>O<sub>2</sub> in mTBI mice was  $268.9\pm 24.3\%$  of that in sham mice ( $^{###}P<0.01$ ); 40 and 100 mg/kg C53N reduced the concentration of H<sub>2</sub>O<sub>2</sub> to  $219.6\pm 32.4\%$  and  $129.0\pm 25.8\%$ , respectively. The concentration of H<sub>2</sub>O<sub>2</sub> was significantly reduced in xyloketal derivative C53N-treated mice compared with vehicle-treated mice at 24 hours post-compression injury ( $^{*}P<0.05$ ,  $^{**}P<0.01$ ). (B) A total GSH assay kit was used to quantify GSH concentration. The concentration of GSH in mTBI mice was  $68.4\pm 15.7\%$  of that in sham mice ( $^{###}P<0.01$ ); 40 and 100 mg/kg C53N reduced the concentration of GSH to  $82.0\pm 7.7\%$  and  $92.7\pm 6.6\%$ , respectively. Upregulated GSH was found in xyloketal derivative C53N-treated mice compared with sham mice ( $^{*}P<0.05$ ). All results are representative of  $n=5-7$  animals per group.

**Abbreviations:** GSH, glutathione; mTBI, mild form of traumatic brain injury.



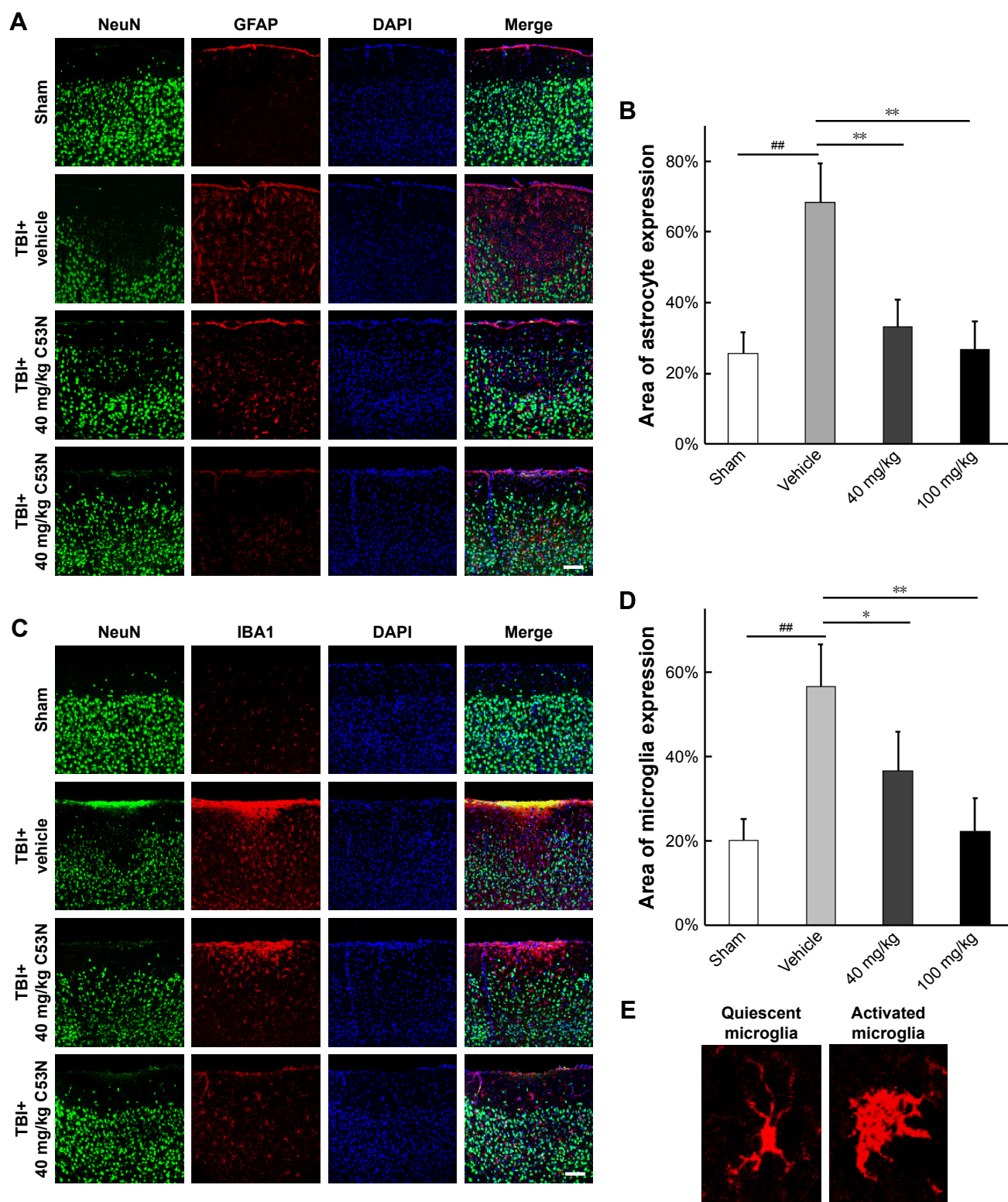


**Figure 7** Astrocyte and microglial measurements 24 hours after compression injury.

**Notes:** (A) Immunohistochemical analyses of astrocytes (GFAP, red) in brain sections. Scale bar: 100  $\mu$ m for A. (B) The percent area containing astrocytes (percent of area with GFAP expression) was quantified; this was 68.4% $\pm$ 11.0% in mTBI mice compared with 25.6% $\pm$ 6.1% in sham mice ( $^{###}P<0.01$ ), while administration of 40 or 100 mg/kg xyloketal derivative C53N significantly decreased the area to 33.2% $\pm$ 7.6% and 26.6% $\pm$ 8.0%, respectively ( $^{**}P<0.01$ ). (C) Immunohistochemical analyses of microglia (Iba1, red) in brain sections. Scale bar: 100  $\mu$ m for C. (D) The percent area containing microglia (percent of area with Iba1 expression) was quantified; this was 56.2% $\pm$ 9.8% in mTBI mice compared with 20.0% $\pm$ 5.4% in sham mice ( $^{###}P<0.01$ ), while administration of 40 mg/kg xyloketal or 100 mg/kg derivative C53N decreased the area to 36.6% $\pm$ 9.2% and 22.2% $\pm$ 7.8%, respectively ( $^{*}P<0.05$ ,  $^{**}P<0.01$ ). (E) In the mTBI-vehicle group, microglia changed their morphology from a quiescent to an activated state, assuming an amoeboid shape.

**Abbreviations:** mTBI, mild form of traumatic brain injury; TBI, traumatic brain injury.



sophisticated functional test may be needed to score mice when using this model.

TBI induces a complex reaction that can result in permanent damage and neurological dysfunction. Cell death is one of the most common outcomes of brain injury. The nucleic acid stain, PI, has been widely used as a simple and reliable technique for real-time monitoring of dead cells<sup>8</sup> and pathological assessment of infarct size. In the present study, we used PI staining to monitor the injury in the compressed site *in vivo* within 12 hours of mTBI, visualized with a two-photon microscope. We found that mTBI gradually increased parenchymal cell death over the 12-hour period. Consistently, a large number of neurons were lost in the PI-stained area 24 hours after TBI, but mice treated with 40 or 100 mg/kg of xyloketal derivative C53N showed a significantly reduced amount of parenchymal neuron death in the acute stage of TBI.

Oxidative stress plays a critical role in the pathophysiology of TBI.<sup>20,21</sup> The severity of TBI-induced brain damage has been directly linked to the degree of oxidative stress, whereas inhibition of oxidative stress can significantly reduce brain damage and improve the outcomes of TBI.<sup>22,23</sup> Oxidative stress may result from an imbalance between pro-oxidant and antioxidant systems caused by either excessive production of ROS or depletion of GSH.<sup>24</sup> GSH is a major cellular non-enzymatic antioxidant that prevents mammalian cells from oxidative damage, while depletion of GSH is an important mechanism for the induction of apoptosis.<sup>25</sup> Our previous studies demonstrated that xyloketal B and its derivative have an excellent antioxidant effect. In the present study, xyloketal derivative C53N significantly reduced the concentration of ROS, but increased the concentration of GSH, indicating that the C53N derivative still maintained good antioxidant activity to protect against mTBI.

Glial cells are the most abundant brain cells and account for over 70% of the brain tissue. Physiologically, glial cells maintain homeostasis of the brain by providing support and recycling waste products. However, glial cells can be harmful under pathological conditions. For example, astrocytes, the most common brain glial cells, have been reported to be involved in different neurological diseases. Furthermore, microglia, the key cells in the brain's innate immune system, can mediate immune responses by releasing proinflammatory cytokines.<sup>26</sup> It has been reported that microglia and astrocytes are the major glial cells involved in immune reactivity and inflammation in the brain.<sup>27</sup> The inflammatory response, including activated astrocyte infiltration (astrogliosis) and

microglial activation (microgliosis) at the site of injury, has been well documented in TBI.<sup>8</sup> Following TBI, reactive astrocytes participate in the inflammatory response by activation of inflammatory pathways, which leads to secretion of different chemokines/cytokines.<sup>28</sup> Similarly, TBI activates the M1 subtype of non-phagocytic microglia during the acute stage to induce neuronal apoptosis.<sup>29</sup> In the present study, activated astrocytes and microglia increased at 24 hours after mTBI. However, treatment with the xyloketal derivative C53N 1 hour after TBI evidently decreased the induction of activated astrocytes and microglia.

In the present study, we investigated the effectiveness of different concentrations of C53N on mTBI only at one intervention time point (1 hour after TBI), which indicated a protective effect in the acute stage of TBI. To be more practical for clinical use, it will be interesting and essential to study the time window of C53N and its long-term protective effects.

## Conclusion

In summary, we tested protection by the xyloketal derivative C53N in a closed-skull mTBI model and showed that the treatment significantly decreased the water content, oxidative stress, and glial reactivity, thereby attenuating parenchymal cell death in the acute phase after compression injury. Thus, the present study highlights the therapeutic potential of xyloketal derivative C53N as a pharmacological intervention for mTBI.

## Acknowledgments

This work was supported by grants from the National Key Clinical Department and Key Discipline of Neurology, Guangdong Provincial Key Laboratory for Diagnosis and Treatment of Major Neurological Diseases (No 2017B030314103), the Southern China International Cooperation Base for Early Intervention and Functional Rehabilitation of Neurological Diseases (No 2015B050501003), Guangdong Provincial Engineering Center for Major Neurological Disease Treatment, Guangdong Provincial Science and Technology Plan Project (No 2016B030230002; No 2017A040406007), the Science and Technology Planning Project of Guangzhou (No 201605030012; No 201604020010), and the Natural Science Foundation of Guangdong Province, People's Republic of China (No 2017A030313064). We also thank Ann Turnley, PhD, from Liwen Bianji, Edanz Group China, for editing the English text of a draft of this manuscript.

## Disclosure

The authors report no conflicts of interest in this work.

## References

- Rosenfeld JV, Maas AI, Bragge P, Morganti-Kossmann MC, Manley GT, Gruen RL. Early management of severe traumatic brain injury. *Lancet*. 2012;380(9847):1088–1098.
- Corrigan JD, Hammond FM. Traumatic brain injury as a chronic health condition. *Arch Phys Med Rehabil*. 2013;94(6):1199–1201.
- Wible EF, Laskowitz DT. Statins in traumatic brain injury. *Neurotherapeutics*. 2010;7(1):62–73.
- Plassman BL, Havlik RJ, Steffens DC, et al. Documented head injury in early adulthood and risk of Alzheimer's disease and other dementias. *Neurology*. 2000;55(8):1158–1166.
- Fehily B, Fitzgerald M. Repeated mild traumatic brain injury: potential mechanisms of damage. *Cell Transplant*. 2017;26(7):1131–1155.
- Abdul-Muneer PM, Chandra N, Haorah J. Interactions of oxidative stress and neurovascular inflammation in the pathogenesis of traumatic brain injury. *Mol Neurobiol*. 2015;51(3):966–979.
- Lenzinger PM, Morganti-Kossmann MC, Laurer HL, Mcintosh TK. The duality of the inflammatory response to traumatic brain injury. *Mol Neurobiol*. 2001;24(1–3):169–181.
- Roth TL, Nayak D, Atanasijevic T, Koretsky AP, Latour LL, McGavern DB. Transcranial amelioration of inflammation and cell death after brain injury. *Nature*. 2014;505(7482):223–228.
- Xiong Y, Mahmood A, Chopp M. Animal models of traumatic brain injury. *Nat Rev Neurosci*. 2013;14(2):128–142.
- Adibhatla RM, Hatcher JF. Lipid oxidation and peroxidation in CNS health and disease: from molecular mechanisms to therapeutic opportunities. *Antioxid Redox Signal*. 2010;12(1):125–169.
- Lin Y, Wu X, Feng S, et al. Five unique compounds: xyloketal from mangrove fungus *Xylaria* sp. from the South China Sea coast. *J Org Chem*. 2001;66(19):6252–6256.
- Pettigrew JD, Wilson PD. Synthesis of xyloketal A, B, C, D, and G analogues. *J Org Chem*. 2006;71(4):1620–1625.
- Chen WL, Qian Y, Meng WF, et al. A novel marine compound xyloketal B protects against oxidized LDL-induced cell injury in vitro. *Biochem Pharmacol*. 2009;78(8):941–950.
- Li S, Shen C, Guo W, et al. Synthesis and neuroprotective action of xyloketal derivatives in Parkinson's disease models. *Mar Drugs*. 2013;11(12):5159–5189.
- Liu S, Luo R, Xiang Q, Xu X, Qiu L, Pang J. Design and synthesis of novel xyloketal derivatives and their protective activities against H<sub>2</sub>O<sub>2</sub>-induced HUVEC injury. *Mar Drugs*. 2015;13(2):948–973.
- Zeng Y, Guo W, Xu G, et al. Xyloketal-derived small molecules show protective effect by decreasing mutant Huntingtin protein aggregates in *Caenorhabditis elegans* model of Huntington's disease. *Drug Des Devel Ther*. 2016;10:1443–1451.
- Li ZX, Chen JW, Yuan F, et al. Xyloketal B exhibits its antioxidant activity through induction of HO-1 in vascular endothelial cells and zebrafish. *Mar Drugs*. 2013;11(2):504–522.
- Liang F, Luo C, Xu G, et al. Deletion of aquaporin-4 is neuroprotective during the acute stage of micro traumatic brain injury in mice. *Neurosci Lett*. 2015;598:29–35.
- Wolff RA, Chien GL, van Winkle DM. Propidium iodide compares favorably with histology and triphenyl tetrazolium chloride in the assessment of experimentally-induced infarct size. *J Mol Cell Cardiol*. 2000;32(2):225–232.
- Bayır H, Kochanek PM, Kagan VE. Oxidative stress in immature brain after traumatic brain injury. *Dev Neurosci*. 2006;28(4–5):420–431.
- Hall ED, Vaishnav RA, Mustafa AG. Antioxidant therapies for traumatic brain injury. *Neurotherapeutics*. 2010;7(1):51–61.
- Bains M, Hall ED. Antioxidant therapies in traumatic brain and spinal cord injury. *Biochim Biophys Acta*. 2012;1822(5):675–684.
- Mustafa AG, Wang JA, Carrico KM, Hall ED. Pharmacological inhibition of lipid peroxidation attenuates calpain-mediated cytoskeletal degradation after traumatic brain injury. *J Neurochem*. 2011;117(3):579–588.
- Aquilano K, Baldelli S, Cardaci S, Rotilio G, Ciriolo MR. Nitric oxide is the primary mediator of cytotoxicity induced by GSH depletion in neuronal cells. *J Cell Sci*. 2011;124(Pt 7):1043–1054.
- Fan S, Yu Y, Qi M, et al. P53-mediated GSH depletion enhanced the cytotoxicity of NO in silibinin-treated human cervical carcinoma HeLa cells. *Free Radic Res*. 2012;46(9):1082–1092.
- Gyoneva S, Ransohoff RM. Inflammatory reaction after traumatic brain injury: therapeutic potential of targeting cell–cell communication by chemokines. *Trends Pharmacol Sci*. 2015;36(7):471–480.
- Witcher KG, Eiferman DS, Godbout JP. Priming the inflammatory pump of the CNS after traumatic brain injury. *Trends Neurosci*. 2015;38(10):609–620.
- Laird MD, Vender JR, Dhandapani KM. Opposing roles for reactive astrocytes following traumatic brain injury. *Neurosignals*. 2008;16(2–3):154–164.
- Yang ST, Lin JW, Chiu BY, Hsu YC, Chang CP, Chang CK. Astragaloside improves outcomes of traumatic brain injury in rats by reducing microglia activation. *Am J Chin Med*. 2014;42(6):1357–1370.

### Drug Design, Development and Therapy

### Publish your work in this journal

Drug Design, Development and Therapy is an international, peer-reviewed open-access journal that spans the spectrum of drug design and development through to clinical applications. Clinical outcomes, patient safety, and programs for the development and effective, safe, and sustained use of medicines are the features of the journal, which

Submit your manuscript here: <http://www.dovepress.com/drug-design-development-and-therapy-journal>

Dovepress

has also been accepted for indexing on PubMed Central. The manuscript management system is completely online and includes a very quick and fair peer-review system, which is all easy to use. Visit <http://www.dovepress.com/testimonials.php> to read real quotes from published authors.